

# A Dosimetric Study on Slab-pine-wood-slab Phantom for Developing the Heterogeneous Chest Phantom Mimicking Actual Human Chest

Om Prakash Gurjar<sup>1,2</sup>, Radha Kishan Paliwal<sup>2</sup>, Surendra Prasad Mishra<sup>3</sup>

<sup>1</sup>Roentgen-SAIMS Radiation Oncology Centre, Sri Aurobindo Institute of Medical Sciences, Indore, Madhya Pradesh, <sup>2</sup>Department of Physics, Mewar University, Chittorgarh, Rajasthan, <sup>3</sup>Department of Radiotherapy, Dr. Ram Manohar Lohia Institute of Medical Sciences, Lucknow, Uttar Pradesh, India

## Abstract

The aim is to study the density, isodose depths, and doses at different points in slab-pine-wood-slab (SPS) phantom, solid phantom SP34 (made up of polystyrene), and chest level of actual patient for developing heterogeneous chest phantom mimicking thoracic region of human body. A 6 MV photon beam of field size of 10 cm × 10 cm was directed perpendicular to the surface of computed tomography (CT) images of chest level of patient, SPS phantom, and SP34 phantom. Dose was calculated using anisotropic analytical algorithm. Hounsfield units were used to calculate the density of each medium. Isodose depths in all the three sets of CT images were measured. Variations between planned doses on treatment planning system (TPS) and measured on linear accelerator (LA) were calculated for three points, namely, near slab-pine-wood interfaces (6 and 18 cm depths) and 10 cm depth in SPS phantom and at the same depths in SP34 phantom. Density of pine-wood, SP34 slabs, chest wall, lung, and soft tissue behind lung was measured as 0.329 ± 0.08, 0.999 ± 0.02, 0.898 ± 0.02, 0.291 ± 0.12, and 1.002 ± 0.03 g/cc, respectively. Depths of 100% and 90% isodose curves in all the three sets of CT images were found to be similar. Depths of 80%, 70%, 60%, 50%, and 40% isodose lines in SPS phantom images were found to be equivalent to that in chest images, while it was least in SP34 phantom images. Variations in doses calculated at 6, 10, and 18 cm depths on TPS and measured on LA were found to be 0.36%, 1.65%, and 2.23%, respectively, in case of SPS phantom, while 0.24%, 0.90%, and 0.93%, respectively, in case of SP34 slab phantom. SPS phantom seemed equivalent to the chest level of human body. Dosimetric results of this study indicate that patient-specific quality assurance can be done using chest phantom mimicking thoracic region of human body, which has been fabricated using polystyrene and pine-wood.

**Keywords:** Anisotropic analytical algorithm, heterogeneous chest phantom, isodose curves, pine-wood

Received on: 28-11-2016

Review completed on: 26-03-2017

Accepted on: 26-03-2017

## INTRODUCTION

The current phase of time in the field of radiation therapy is revolutionary period technology wise when day to day new and better radiotherapy machines equipped with different modes of treatment are being introduced, for example, intensity-modulated radiation therapy (IMRT), image-guided radiation therapy, arc therapy, and in recent days, flattening filter-free IMRT. The developments in all these techniques are of special concern with the patient setup accuracy, treatment time, and the dose conformity to the target with precisely saving the organs at risk using multileaf collimators. The treatment planning systems (TPS) are also being developed and upgraded in parallel with these plan-delivering machines. The newly introduced TPS are technically more efficient, fast,

and have more accurate dose-calculating algorithm which enable the users to do planning in short time with enhanced accuracy.

The different tumor sites such as head and neck, oral cavity, lung, breast, and brain have high inhomogeneities and have different radiologic properties.<sup>[1]</sup> The Task Group 65 (TG-65) of the American Association of Physicists in Medicine (AAPM) describes that “the general principle of 3% accuracy in dose

**Address for correspondence:** Dr. Om Prakash Gurjar, Roentgen-SAIMS Radiation Oncology Centre, Sri Aurobindo Institute of Medical Sciences, Indore - 453 111, Madhya Pradesh, India.  
E-mail: ominbarc@gmail.com

### Access this article online

Quick Response Code:



Website:  
www.jmp.org.in

DOI:  
10.4103/jmp.JMP\_125\_16

This is an open access article distributed under the terms of the Creative Commons Attribution-NonCommercial-ShareAlike 3.0 License, which allows others to remix, tweak, and build upon the work non-commercially, as long as the author is credited and the new creations are licensed under the identical terms.

**For reprints contact:** reprints@medknow.com

**How to cite this article:** Gurjar OP, Paliwal RK, Mishra SP. A dosimetric study on slab-pine-wood-slab phantom for developing the heterogeneous chest phantom mimicking actual human chest. *J Med Phys* 2017;42:80-5.

delivery with the corresponding need for better than 2% accuracy in correcting for inhomogeneities is a reasonable, albeit, challenging goal.<sup>[11]</sup>

The crucial component in the TPS is algorithm which should calculate the dose with high accuracy considering the heterogeneity in the media. All algorithms calculate the dose using computed tomography (CT) images and the structures delineated on these CT images. Anisotropic analytical algorithm (AAA) is based on the superposition-convolution method, which calculates the dose by superposition of dose kernels of primary and scatter components that are derived from the Monte Carlo (MC) method.<sup>[2]</sup> The inhomogeneities correction in superposition-convolution method in the AAA is done in the beamlet direction as well as in lateral directions.<sup>[3-6]</sup> But still, it is insufficient to calculate the dose with high accuracy at the cavity–soft tissue interface, especially in the re-build-up region.<sup>[7,8]</sup>

Recently, more advanced algorithm Acuros XB (AXB) (Type C) has been introduced in the Eclipse TPS,<sup>[9]</sup> which uses the linear Boltzmann transfer equation and solves numerically that describes the macroscopic behavior of ionizing particles as they travel through matter and interact with it.<sup>[9]</sup> AXB has been presented to show equivalent accuracy to MC calculation in heterogeneous media.<sup>[10,11]</sup>

Along with accurate dose calculation and good treatment planning, it is also very important to verify this planned dose by delivering the plan on linear accelerator (LA) and measuring the dose using small volume ion chamber and quality assurance (QA) phantom. Use of different QA phantoms of homogeneous density equivalent to that of water, i.e., 1 g/cc is done widely following the AAPM TG Report 120.<sup>[12]</sup> However, doing the patient-specific QA using a homogeneous phantom is not justified as the dose deposition pattern in highly inhomogeneous medium (human body) is totally different from that in a medium having uniform density throughout its volume. The dose deposition is affected by the density variation in the medium specially at the interface of two densities, for example, bone–soft tissue interface and cavity–soft tissue interface.<sup>[13]</sup> Hence calculating dose on CT images of a homogeneous QA phantom and measuring it on LA using the mentioned phantom gives very less error, mostly not more than 1%–2%.<sup>[14]</sup> However, calculating the dose on CT images of a heterogeneous QA phantom and then measuring on LA using the same phantom will yield comparatively higher error,<sup>[14]</sup> which indicates that the algorithm in the TPS is not accurate enough.

Few QA phantoms with the heterogeneous density (anthropomorphic phantom) are commercially available in the field of radiotherapy. However, these phantoms are very costly and most of the radiotherapy centers in developing countries cannot afford to purchase these phantoms due to the cost factor. Therefore, this study has been carried out to fabricate the heterogeneous density QA phantom for the dose verification in the case of chest site radiotherapy plans.

## MATERIALS AND METHODS

Slab-pinewood-slab (SPS) phantom of the dimension  $30 \times 30 \times 29 \text{ cm}^3$  was made using the 15 slabs (each of 1 cm thickness) of “solid phantom SP34 (SP34 phantom)” (IBA Dosimetry GmbH, Schwarzenbruck, Germany) and seven slabs (each of 2 cm thickness) of pinewood. A hole of the chamber size was made in one wood slab for inserting the chamber inside for measurements. The phantom comprised five SP34 slabs at the top, and then seven slabs of pine wood in between and then again ten SP34 slabs at the bottom. Each slab of SP34 phantom is made up of polystyrene  $\text{C}_8\text{H}_8$  (composition: 98% polystyrene + 2%  $\text{TiO}_2$ ) with effective atomic number 5.74.<sup>[15]</sup> The wood slabs were specially designed by cutting the dry light pine wood using the commercial wood cutter machines at wood shop. The density of SP34 phantom slabs is 1.045 g/cc which is equivalent to that of muscle and fat.<sup>[14]</sup> The SPS phantom is shown in Figure 1.

The present study has been done in two parts, first one is the dosimetric study on TPS and the second one is the verification of planned dose on TPS on the CT images of SPS phantom and SP34 phantom by measuring the dose on LA Varian Clinac DMX (Varian Medical Systems, Palo Alto, CA, USA) using SPS and SP34 phantoms. In the first part of the study, CT images of three mediums, namely, thoracic region of actual patient, SPS phantom, and the SP34 phantom as shown in Figure 2 were used. The CT images of thoracic region of the patient already planned were used.

The SPS and SP34 phantoms were scanned on a Siemens SOMATOM Definition AS scanner (Siemens Medical Systems, Germany) and CT images of 3 mm slice thickness were acquired for the planning purpose. In the case of SPS phantom, CT imaging repeated thrice to obtain three sets of CT images by placing the chamber holding slab of pinewood at three different positions, namely, just below

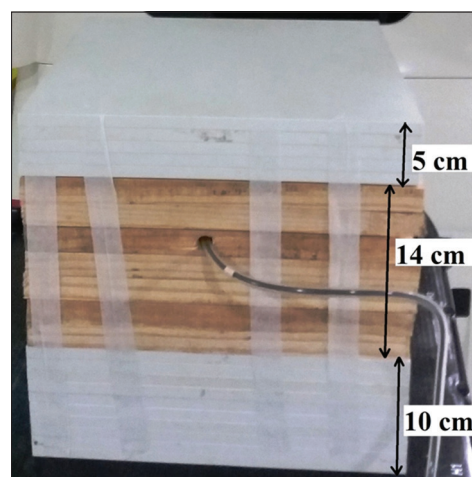


**Figure 1:** Photograph of slab-pinewood-slab phantom of the dimension  $30 \text{ cm} \times 30 \text{ cm} \times 29 \text{ cm}$  consisting of 15 slabs (each of 1 cm thickness) of “solid phantom SP34” and seven slabs (each of 2 cm thickness) of pinewood. Also shown in the figure is the ionization chamber used for measurement

the five SP34, at third position among pine wood slabs, and just above the ten SP34 slabs as shown in Figure 3. The chamber used was a 0.13 cc ionization chamber (IBA Dosimetry, Germany) which is available at our center along with DOSE1 electrometer (IBA Dosimetry, Germany) for dose measurement.

All CT image sets were imported on TPS Eclipse version 8.9 (Varian Medical Systems, Palo Alto, CA, USA). The SP34 slabs were delineated as tissue-equivalent medium and pinewood slabs as lung-equivalent medium. Ion chamber was also delineated to specify the dose at its active volume.

A single beam of 6 MV x-rays of 10 cm × 10 cm field size was directed on to the chest wall, SPS phantom, and SP34 phantom perpendicular to the surface with source-to-surface distance of 100 cm. The dose was calculated using AAA version 8.9.08 with a grid size of 0.25 cm.

The density of pinewood, SP34 phantom, chest wall, lung, and soft tissue behind the lung was measured with the help of Hounsfield unit (HU) measured from CT images on TPS by HU tool, and the HU-density conversion formula

$$H = 1000 \left( \frac{\rho}{\rho_w} - 1.0 \right) \text{.}^{[14]}$$

In addition, the physical density of pinewood was measured by weighing one slab of dimension of 30 × 30 × 2 cm<sup>3</sup>.

The isodose curves of 100%, 90%, 80%, 70%, 60%, 50%, and 40% were measured in all the three CT image data sets and

compared. Furthermore, the point doses at the depth of 6 cm, 10 cm, and 18 cm in the CT images of SPS phantom were noted from the TPS. 6 and 18 cm were chosen as each pinewood slab is 2 cm thick, and cavity prepared in one slab for the insertion of chamber is at the center of a slab, therefore placing this wood slab just below the first five SP34 slabs would bring the ion chamber at 6 cm depth from the surface of SPS phantom; similarly on placing this wood slab having ion chamber just above the last ten SP34 slabs would bring the chamber at 18 cm from the surface of SPS phantom.

The SPS phantom along with ion chamber was set on LA couch and a cone-beam CT was acquired with the Varian On-Board-Imaging system consisting of a 125 kVp X-ray tube isocentrically mounted to the gantry of the accelerator. Setup accuracy of SPS phantom and the ion chamber inside it was verified by standard procedure using the anatomy-matching software (Varian portal Vision 7.5).<sup>[16]</sup> After verifying the setup, doses at all the three points were measured and compared with the planned doses at the concerned points.

## RESULTS

The density of pinewood, SP34 slabs, chest wall, lung, and soft tissue behind the lung was measured as 0.329 ± 0.08, 0.999 ± 0.02, 0.898 ± 0.02, 0.291 ± 0.12, and 1.002 ± 0.03 g/cc, respectively. The HU and density for all the five mediums are shown in Table 1. The physical density of pinewood measured by weighing one slab was found to be 0.304 g/

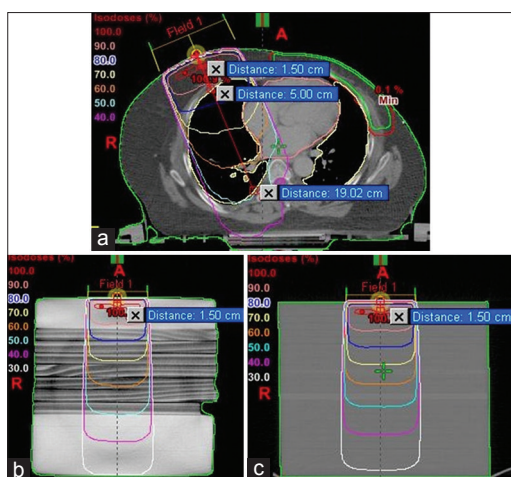


**Figure 2:** Isodose lines in the computed tomography slice at (a) chest level of patient, (b) middle of slab-pinewood-slab phantom, and (c) middle of slab phantom

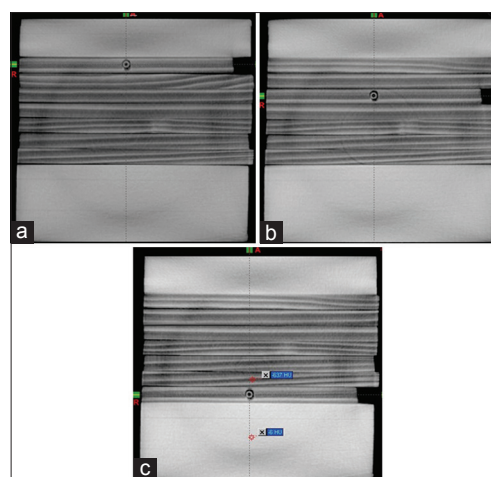


**Figure 3:** Computed tomography slices of slab-pinewood-slab phantom having ion chamber at (a) 6 cm depth (1 cm below the five SP34), (b) 10 cm depth, and (c) 18 cm depth (1 cm above the last ten SP34 slabs)

**Table 1: Measured Hounsfield unit and density of chest wall, lung, soft tissue back to lung, pinewood, and SP34 slab phantom**

Parameters	HU of pinewood slabs	HU of SP34 slabs	HU of chest wall	HU of lung	HU of soft tissue behind the lung
Mean HU	-670.9±83.57	-1.2±20.06	-101.8±16.03	-708.9±119.13	1.7±31.31
Density (g/cc)	0.329±0.08	0.999±0.02	0.898±0.02	0.291±0.12	1.002±0.03

HU: Hounsfield unit

cc. The total weight of  $30 \times 30 \times 2 \text{ cm}^3$  pinewood slab was measured as 547 g.

The depths of 100% and 90% isodose curves in SPS phantom, SP34 phantom, and actual patient chest level were found to be similar. The depths of 80%, 70%, 60%, and 50% isodose curves in SPS phantom are little lesser as compared to that in actual patient chest level, while it is least in CT images of SP34 phantom. The depth of 40% isodose curve is highest in SPS phantom than little lesser in actual patient chest level and least in SP34 phantom. The detailed results of the measurements of isodose depths are shown in Table 2.

The variations in the doses calculated on TPS at 6 cm, 10 cm, and 18 cm depths and measured on LA in the SPS phantom were found to be 0.36%, 1.65%, and 2.23%, respectively. Similarly, the variations in the case of SP34 slab phantom were

found to be 0.24%, 0.90%, and 0.93%. The detailed results are shown in Table 3.

## DISCUSSION

The recent developments in the dose-calculating algorithms have improved the accuracy in dose calculation, however doing the patient-specific QA is mandatory to make sure that the planned dose and the delivered dose in the same medium are within the tolerance limit, i.e., <3% as mentioned in the International Commission on Radiation Units and Measurements 83 (ICRU 83).<sup>[17]</sup> The ICRU 83 published in 2010 propounds that the biggest causes of treatment failures are geographical miss due to inaccurate target delineation and dosimetric variation more than 3%.<sup>[14]</sup> Therefore, along with the developments in dose-calculating algorithms, it is also equally important to use the QA phantoms which should have heterogeneity pattern inside same as in human body and the phantom should mimic the actual human body. Since calculating the dose accurately in a simple and homogeneous medium is easy for algorithm, it becomes tedious in a complex heterogeneous density medium.

This study has been carried out to study the density pattern and dose distribution pattern in the chest-level CT images having chest wall, lung, and soft tissue behind the lung. These patterns were compared with that on the CT images of SPS and SP34 slab phantoms. The CT image of the chest wall at beam isocenter had chest wall of 5 cm, lung of 14 cm, and the soft tissue behind the lung of 10 depths at the beam center. The SPS phantom had 5 cm SP34 slabs (five slabs each of 1 cm thickness), 14 cm pinewood slabs (seven slabs each of 2 cm thickness), and 10 cm of SP34 slabs. The measured density of chest wall ( $0.898 \pm 0.02 \text{ g/}$

**Table 2: Depths of relative dose values in computed tomography images of chest level of actual patient, slab-pine-wood-slab phantom, and SP34 phantom**

Isodose lines (%)	Isodose depth in SPS phantom (cm)	Isodose depth in SP34 phantom (cm)	Isodose depth in patient (cm)
100	1.5	1.5	1.5
90	4.15	4.19	4.22
80	7.10	6.43	7.23
70	10.55	9.00	11.84
60	14.72	11.79	16.34
50	19.17	15.05	19.57
40	24.04	18.99	23.66

SPS: Slab-pine-wood-slab

**Table 3: A comparison of TPS calculated doses and corresponding measured doses in SPS phantom for 6 MV x-rays**

MU	SPS phantom								
	Dose (cGy) at								
	6 cm depth (1 cm below slab-pine-wood interface)			10 cm depth (5 cm in pinewood)			18 cm depth (1 cm above pinewood-slab interface)		
	Planned on TPS	Measured on LA	Percentage of variation	Planned on TPS	Measured on LA	Percentage of variation	Planned on TPS	Measured on LA	Percentage of variation
100	84.1	83.8	-0.36	72.6	73.8	1.65	53.7	54.9	2.23
200	168.2	167.6	-0.36	145.2	147.6	1.65	107.4	109.8	2.23
300	252.3	251.4	-0.36	217.8	221.4	1.65	161.1	164.7	2.23
Mean			-0.36			1.65			2.23
MU	SP34 phantom								
	Dose (cGy) at								
	6 cm depth			10 cm depth			18 cm depth		
	Planned on TPS	Measured on LA	Percentage of variation	Planned on TPS	Measured on LA	Percentage of variation	Planned on TPS	Measured on LA	Percentage of variation
100	81.7	81.9	0.24	66.5	67.1	0.90	42.8	43.2	0.93
200	163.4	163.8	0.24	133.0	134.2	0.90	85.6	86.4	0.93
300	245.1	245.7	0.24	199.5	201.3	0.90	128.4	129.6	0.93
Mean			0.24			0.90			0.93

TPS: Treatment planning systems, LA: Linear accelerator, SPS: Slab-pine-wood-slab, MU: Monitoring units

cc) and soft tissue behind the lung ( $1.002 \pm 0.03$  g/cc) is near to that of SP34 slabs ( $0.999 \pm 0.02$  g/cc), also the density of lung ( $0.291 \pm 0.12$  g/cc) is approximately equivalent to that of pinewood slabs ( $0.329 \pm 0.08$  g/cc). Therefore, using SPS phantom for the QA of plans done for chest site of the patients is rational.

The density of chest wall and tissue behind the lung concurred with the density of soft tissues as mentioned in the literature.<sup>[18,19]</sup> The physical density of the lung mentioned in the literature varies between 0.2 and 0.5 g/cc during the respiration,<sup>[20]</sup> therefore density measured in this study is correct. The measured density of the SP34 slab phantom concurred with the value mentioned in the literature.<sup>[15]</sup> The radiological properties of the kailwood is equivalent to that of lung medium, also the electron densities in both the mediums are equivalent.<sup>[21]</sup> However, due to unavailability of the kailwood, pinewood has been used in this study as it is also having low density equivalent to that of lung.

The isodose depths on the CT images of all the three mediums, namely, chest level of the patient, SPS phantom, and SP34 phantom are approximately same for 100% and 90% isodose curves. However, 90% isodose depth in chest is higher than that in both the phantoms as its density is slightly lesser than that of slab, also the 90% isodose depth in SPS phantom is lesser than that in SP34 phantom as the number of backscattered electrons in SPS phantom at slab-kailwood interface is lesser. The depth of the isodose curves in all the three mediums goes on increasing from 80% to 40%, although the depth of the same isodose curve in all the three mediums varied significantly. The depth of each isodose curve from 80% to 50% is highest in CT image of chest, then in CT image of SPS phantom, and then in CT images of SP34 phantom. The variation in the depths of same isodose curves in the CT image of chest and that of SPS phantom is due to the slightly lesser density of the lung as compared to that of pinewood, also the varying thickness of the lung and uniform thickness of the pinewood across the field are other factors for this difference. Forty percent isodose depth in SPS phantom is higher than that in chest level of patient as the density of soft tissue behind the lung is higher in comparison to that of SP34 slabs.

Most of the radiotherapy centers in developing countries use slab phantom of 30 cm × 30 cm × 30 cm size for patient-specific QA; for this purpose, all the beams are set to gantry angle 0° on TPS while making the QA plan, so because of the simpler medium of the phantom, i.e., similar density throughout its volume, QA results are always achieved well within the tolerance limits, i.e., <3%.<sup>[17]</sup> In the current study, similar results have been observed, variation in the planned and measured doses at all the three points is <1%. Hence, using the phantom of same density throughout its volume for the QA of plans done on different heterogeneous body sites of patient is not rational.

The variation in the doses calculated near the interface regions (6 cm and 18 cm depths in SPS phantom) and in 5 cm depth of pinewood (10 cm depth in SPS phantom) and

measured doses at the same points using SPS phantom on the LA gave slightly different results. It is -0.36% for the point at “slab–pinewood” interface, + 2.23% for the point at “pinewood–slab” interface, and + 1.65% for the point at 5 cm depth in pinewood, i.e., 10 cm depth from the surface of SPS phantom. These results concurred with the theory of dose deposition mechanism at the interface regions of two different density media which is as follows:<sup>[13,22]</sup>

### Soft tissue–air cavity interface

As the density of soft tissue is higher than that of air cavity, when beam is incident, then higher number of secondary electrons is produced in soft tissue, the number of scattering back electrons at interface region in the air cavity will be lesser, therefore lesser dose will be deposited at the interface.

### Air cavity–soft tissue interface

Since the density of air cavity is lesser than that of soft tissue, lesser number of secondary electrons is produced, and when they travel toward air cavity–soft tissue interface, the number of scattering back electrons increases at interface region.

Hence, along with the improvement in the dose calculation algorithms, it is also equally important to use the heterogeneous body phantoms for patient-specific dosimetry which would mimic the actual human body. This study clearly finds that the SPS phantom is better to use for the patient-specific QA when compared to the SP34 slab phantom.

It will be good if the chest phantom in the same shape as that of actual human chest is prepared using pinewood or any other material of equivalent density to form lung, polystyrene C<sub>8</sub>H<sub>8</sub> (composition: 98% polystyrene + 2% TiO<sub>2</sub>) to form soft tissue, and suitable material to form ribs and spine.

## CONCLUSIONS

The results of this study on the density measurement and depth of isodose curves indicate that SPS phantom represents the chest level of human body in better way as compared to SP34 slab phantom. In addition, the point dose measurements at the interface regions and 5 cm depth in pinewood indicate that the use of heterogeneous phantom of the same density pattern as that of actual human body site should be done for verifying the dose calculated by the algorithm. It can be concluded that SPS phantom is a better option for patient-specific QA, however along with density patterns, the phantom in the same shape and size as that of actual human chest level will be the good phantom for more accurate dose verification.

### Financial support and sponsorship

Nil.

### Conflicts of interest

There are no conflicts of interest.

## REFERENCES

1. Papanikolaou N, Battista J, Mackie T, Kappas C, Boyer A. Tissue Inhomogeneity Corrections for Megavoltage Photon Beams. AAPM

- Report No. 85, Task Group No. 65; 2004.
2. Rana S. Clinical dosimetric impact of Acuros XB and analytical anisotropic algorithm (AAA) on real lung cancer treatment plans: Review. *Int J Cancer Ther Oncol* 2014;2:02019.
  3. Gagné IM, Zavgorodni S. Evaluation of the analytical anisotropic algorithm in an extreme water-lung interface phantom using Monte Carlo dose calculations. *J Appl Clin Med Phys* 2006;8:33-46.
  4. Sievinen J, Ulmer W, Kaissl W. AAA photon dose calculation Model in Eclipse. Palo Alto, CA: Varian Medical Systems; 2005.
  5. Ulmer W, Pyyry J, Kaissl W. A 3D photon superposition/convolution algorithm and its foundation on results of Monte Carlo calculations. *Phys Med Biol* 2005;50:1767-90.
  6. Tillikainen L, Helminen H, Torsti T, Siljamäki S, Alakuijala J, Pyyry J, *et al.* A 3D pencil-beam-based superposition algorithm for photon dose calculation in heterogeneous media. *Phys Med Biol* 2008;53:3821-39.
  7. Van Esch A, Tillikainen L, Pyykkonen J, Tenhunen M, Helminen H, Siljamäki S, *et al.* Testing of the analytical anisotropic algorithm for photon dose calculation. *Med Phys* 2006;33:4130-48.
  8. Aarup LR, Nahum AE, Zacharou C, Juhler-Nøttrup T, Knöös T, Nyström H, *et al.* The effect of different lung densities on the accuracy of various radiotherapy dose calculation methods: Implications for tumour coverage. *Radiother Oncol* 2009;91:405-14.
  9. Vassiliev ON, Wareing TA, McGhee J, Failla G, Salehpour MR, Mourtada F. Validation of a new grid-based Boltzmann equation solver for dose calculation in radiotherapy with photon beams. *Phys Med Biol* 2010;55:581-98.
  10. Fogliata A, Nicolini G, Clivio A, Vanetti E, Cozzi L. Dosimetric evaluation of Acuros XB Advanced dose calculation algorithm in heterogeneous media. *Radiat Oncol* 2011;6:82.
  11. Bush K, Gagne IM, Zavgorodni S, Ansbacher W, Beckham W. Dosimetric validation of Acuros XB with Monte Carlo methods for photon dose calculations. *Med Phys* 2011;38:2208-21.
  12. Low DA, Moran JM, Dempsey JF, Dong L, Oldham M. Dosimetry tools and techniques for IMRT. *Med Phys* 2011;38:1313-38.
  13. Broerse JJ, Zoetelief J. Dose inhomogeneities for photons and neutrons near interfaces. *Radiat Prot Dosimetry* 2004;112:509-17.
  14. Gurjar OP, Mishra SP, Bhandari V, Pathak P, Patel P, Shrivastav G. Radiation dose verification using real tissue phantom in modern radiotherapy techniques. *J Med Phys* 2014;39:44-9.
  15. Christ G. White polystyrene as a substitute for water in high energy photon dosimetry. *Med Phys* 1995;22:2097-100.
  16. Gurjar OP, Mishra SP, Bhandari V, Pathak P, Pant S, Patel P. A study on the necessity of kV-CBCT imaging compared to kV-orthogonal portal imaging based on setup errors: Considering other socioeconomic factors. *J Cancer Res Ther* 2014;10:583-6.
  17. ICRU Report 83. Prescribing, Recording, and Reporting Photon-Beam Intensity-Modulated Radiation Therapy (IMRT). International Commission on Radiation Units and Measurements, Bethesda; 2010.
  18. Khan FM. *The Physics of Radiation Therapy*. 4<sup>th</sup> ed. Philadelphia: Lippincott Williams and Wilkins; 2010.
  19. Attix FH. *Introduction to Radiological Physics and Radiation Dosimetry*. Hoboken: John Wiley and Sons; 1986.
  20. Ravikumar B, Lakshminarayana S. Determination of the tissue inhomogeneity correction in high dose rate brachytherapy for iridium-192 source. *J Med Phys* 2012;37:27-31.
  21. Kumar A, Sharma SD, Arya AK, Gupta S, Shrotriya D. Effect of low-density heterogeneities in telecobalt therapy and validation of dose calculation algorithm of a treatment planning system. *J Med Phys* 2011;36:198-204.
  22. Binger T, Seifert H, Blass G, Bormann KH, Rücker M. Dose inhomogeneities on surfaces of different dental implants during irradiation with high-energy photons. *Dentomaxillofac Radiol* 2008;37:149-53.